Table I.

Starting Ester	Silyl Ynol Ether (time/yield)[a,b]
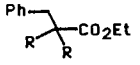 5a (R=H) 5b (R=Me)	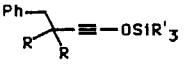 6a (1.5 hr/66%) 6b (18 hr/71%)
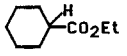 7	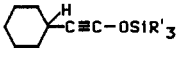 8 (3.5 hr/68%)
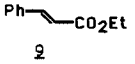 9	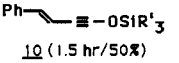 10 (1.5 hr/50%)
Ph−CO2Et 11	Ph−C≡C−OSiR'3 12[5a] (1.5 hr/63%)
 13	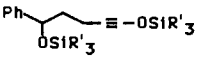 14 (24 hr/74%)

[a] R' = *i*-Pr. [b] Silylation time/yield of purified material after flash chromatography; satisfactory analytical and spectral data for all products is presented in the supplementary material.

the synthesis of these little-studied intermediates.

Along with the fact that silyl ynol ethers can now be easily prepared, we would also like to report that they can be cleaved by methyllithium to afford clean solutions of lithium ynolate anions. Both the triisopropylsilyl ynol **6a** and the *tert*-butyldimethylsilyl ynol **16** afforded the ynolate **15** with methyllithium in THF at room temperature. As expected, **6a** was cleaved more slowly than **16** (3.5 h vs. 30 min), but both afforded high yields of ynolate **15** as evidenced by silylation to the other silyl ynol ether (i.e., **6a** afforded **16** in 93% yield while **16** afforded **6a** in 92% yield). Silyl ynol **6a** was shown to be unchanged after a period

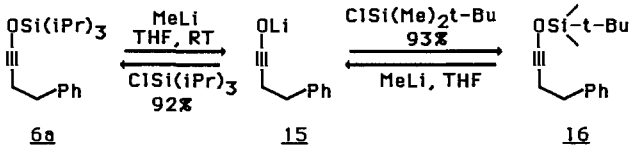

of 2 weeks in hexane solution, and so these ethers effectively offer a means of "storing" ynolate anions, much as silyl enol ethers can be used to "store" ketone enolate anions. This ability to interconvert ynol silyl ethers and ynolate anions, coupled with their direct synthesis from simple ester precursors, now makes the study and utilization of these materials a much easier task. We are continuing to pursue the chemistry of ynolate anions and silyl ynol ethers in our labs.

Acknowledgment. We thank Walter Johnson, of Analytical, Physical and Structural Chemistry at SK&F, for high-resolution mass spectra.

Supplementary Material Available: IR, NMR, and high-resolution mass spectral data for **6a,b**, **8**, **10**, **12**, **14**, and **16** (1 page). Ordering information is given on any current masthead page.

Reactions of Gas-Phase Dipositive Titanium Ions with Alkanes

Russ Tonkyn and James C. Weisshaar*

Department of Chemistry
University of Wisconsin—Madison
Madison, Wisconsin 53706

Received June 25, 1986

The chemical reactions of gas-phase atomic metal cations M^+,[1] metal cluster ions M_n^+,[2] mixed-metal cluster ions such as $FeCo^+$,[3] atomic metal anions M^-,[4] and metal anion complexes[5] are remarkable in their diversity. Here we report the first reactivity studies of a *dipositive* transition-metal ion, namely, Ti^{2+}. This is a highly energetic, open-shell species whose second ionization energy of 13.58 eV[6] exceeds the first ionization energy of most organic neutrals. The chemistry of Ti^{2+} with small alkanes in 0.4 torr of He is remarkably selective. The dominant reaction paths are completely different for CH_4 (collisional stabilization of dipositive adduct ions), C_2H_6 (hydride ion abstraction), and C_3H_8 (electron transfer).

The experiments are carried out in a fast flow reactor[7] equipped with a laser vaporization source of metal ions upstream; neutral reagent inlets for addition of small, calibrated flows of reactant gas midstream; and a quadrupole mass spectrometer which samples the flow through a 1-mm pinhole in a Mo disk downstream. For He buffer gas pressures below about 0.5 torr, we find that a Ti metal target produces Ti^{2+} ions almost exclusively, while at higher pressure Ti^+ becomes the dominant ion.[8] No Ti^{n+}, $n \geq 3$, is observed; if such species are created, they can charge transfer with He. Product ion mass spectra were obtained at alkane flows sufficiently small that the branching of the primary Ti^{2+} reaction is not perturbed by secondary reactions. The detection is about 5 times more sensitive to +2 ions than to +1 ions, so that total detected signal diminishes in reactions leading to +1 ions. Reaction rate constants were obtained from the logarithmic decay of the Ti^{2+} signal vs. calibrated alkane flow at fixed reaction length of 42 cm.[7]

Figure 1 shows the Ti^{2+} + alkane product ion mass spectra. All exothermic product channels form at least one Ti-containing ion whose charge and mass are directly determined.[9] The corresponding neutral and hydrocarbon ion products are inferred. Interference from alkane reactions with He^+, He_2^+, and metastable He* (2^3S, 2^1S) created in the source produces large hydrocarbon ion signals which preclude direct determination of hydrocarbon ion products from the Ti^{2+} reactions. The only Ti^{2+} + CH_4 primary product definitely observed is the collisionally stabilized adduct ion $TiCH_4^{2+}$. Experiments at lower CH_4 pressure than used in Figure 1 show that ≥80% of the primary product is the adduct ion; small Ti^+ or TiH^+ signals (≤20%) could be obscured by higher cluster ions at m/q = 48 and 49. Additional sequential reactions form larger dipositive adduct ions $Ti(CH_4)_n^{2+}$, $n \leq 4$. The n = 4 species is relatively inert to further CH_4 addition. Impurity H_2O can readily substitute for at least one CH_4 unit in all of the adducts. The Ti^{2+} + C_2H_6 reaction yields the H^-

(1) See, for example: Allison, J.; Ridge, D. P. *J. Am. Chem. Soc.* **1979**, *101*, 4998. Peake, D. A.; Gross, M. L.; Ridge, D. P. *J. Am. Chem. Soc.* **1984**, *106*, 4307. Mandich, M. L.; Halle, L. F.; Beauchamp, J. L. *J. Am. Chem. Soc.* **1984**, *106*, 4403. Elkind, J. L.; Armentrout, P. B. *J. Phys. Chem.* **1985**, *89*, 5626. Jacobson, D. B.; Freiser, B. S. *J. Am. Chem. Soc.* **1983**, *105*, 7484. Jones, R. W.; Staley, R. H. *J. Am. Chem. Soc.* **1982**, *104*, 1235 and references therein.

(2) Hanley, L.; Anderson, S. L. *Chem. Phys. Lett.* **1985**, *122*, 410. Ervin, K.; Loh, S. K.; Aristov, N.; Armentrout, P. B. *J. Phys. Chem.* **1983**, *87*, 3593.

(3) Jacobson, D. B.; Freiser, B. S. *J. Am. Chem. Soc.* **1984**, *106*, 5351; **1985**, *107*, 1581.

(4) Sallans, L.; Lane, K.; Squires, R. R.; Freiser, B. S. *J. Am. Chem. Soc.* **1983**, *105*, 6352. Sallans, L.; Lane, K. R.; Squires, R. R.; Freiser, B. S. *J. Am. Chem. Soc.* **1985**, *107*, 4379.

(5) Lane, K. R.; Squires, R. R. *J. Am. Chem. Soc.* **1985**, *107*, 6402. McDonald, R. N.; Chowkhury, A. K.; Jones, M. T. *J. Am. Chem. Soc.* **1986**, *108*, 3105.

(6) Moore, C. E. *Atomic Energy Levels*; N.B.S. Circular No. 467: Washington, DC, 1949.

(7) Tonkyn, R.; Weisshaar, J. C. *J. Phys. Chem.* **1986**, *90*, 2305. Tonkyn, R.; Weisshaar, J. C., unpublished results.

(8) It appears that the target produces predominantly Ti^{2+} when embedded in He, perhaps because the metastable He* (2^1S) state at 20.6 eV and He^+ at 24.6 eV both have sufficient energy to *doubly* ionize Ti. The sum of the first two ionization energies of Ti is 20.4 eV. We suggest that above 0.5 torr, the ablated material is confined to sufficiently small volume that Ti^{2+} + Ti → $2Ti^+$ is efficient, whereas below 0.5 torr the Ti^{2+} ions escape the source region without colliding with a neutral Ti atom. There is some evidence that Ti^+ is lost more rapidly by diffusion than is Ti^{2+}.

(9) The stable Ti isotopes (natural abundances) are m/q = 46 (7.9%), 47 (7.3%), 48 (73.9%), 49 (5.5%), and 50 (5.3%). We typically do not entirely resolve the 2+ ion pattern centered at m/q = 24. The isotope pattern precludes the remote possibility of contamination of Mg^+ ions at m/q = 24.

0002-7863/86/1508-7128$01.50/0

Table I. Ti^{2+} + RH Reaction Rates, Product ΔH's, and Curve Crossing Points

RH	k,[a] 10^{-9} $cm^3\ s^{-1}$	primary prod, % yield	$\Delta H(Ti^+ + RH^+)$,[b] eV	r^*, Å	$\Delta H(TiH^+ + R^{\cdot+})$,[b] eV	r', Å
CH_4	0.29 ± 0.13	$TiCH_4^{2+}$ (≥80%)	−1.0	14.4	−1.6	9.1
C_2H_6	2.8 ± 0.8	TiH^+ (≥90%)	−2.1	7.0	−3.4	4.6
C_3H_8	2.6 ± 0.8	Ti^+ (≥70%)	−2.5	6.1	−3.6 (−4.3)	4.5 (4.0)

[a] From pseudo-first-order measurements of Ti^{2+} decay vs. alkane flow at fixed reaction length of 42 cm. T = 300 K and P_{He} = 0.38 torr. The CH_4, C_2H_6, and C_3H_8 Langevin collision rates with a 2+ ion are in the range (2.2–2.4) × 10^{-9} $cm^3\ s^{-1}$. For the termolecular Ti^{2+} + CH_4 association, the "effective bimolecular rate constant" reported is the rate constant for bimolecular collisions which lead to collisionally stabilized adduct ions at 0.38 torr of He. See ref 7. [b] Ti and RH ionization energies from ref 6 and 17. $D^0(Ti^+–H)$ = 55 kcal/mol.[18] ΔH_f° of alkyl ions from ref 19. Values for n-$C_3H_7^+$ and i-$C_3H_7^+$ given without and with parentheses. [c] One-dimensional curve crossing points for electron transfer (r^*) and H^- transfer (r'), calculated by equating $V_1(r)$ with $V_2(r)$ + ΔH. See text.

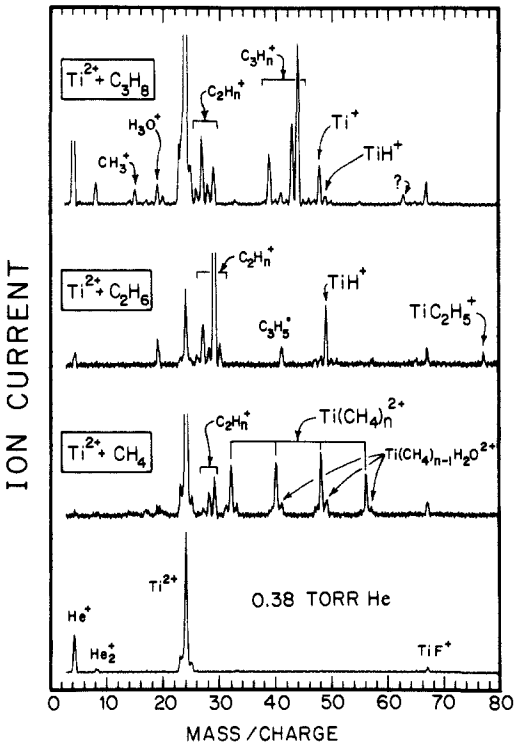

Figure 1. Mass spectra of Ti^{2+} reactants in 0.38 torr of He (bottom) and of product ions resulting from addition of small flows of CH_4, C_2H_6, and C_3H_8. Vertical scales are not related. Most of the C_1, C_2, and C_3 products arise from reactions with He^+, He_2^+, and He* (2^3S) formed in the source. Ti-containing products are clearly identifiable by the isotope pattern[9] as 2+ or 1+ ions, as labeled. The detection is about 5 times more sensitive to 2+ ions than to 1+ ions. Impurity peaks are due to H_2O and SF_6, the latter added in minute flows to attach electrons. The m/q = 63 peaks labeled "?" is not $TiCH_3^+$, since it lacks the proper isotope pattern.

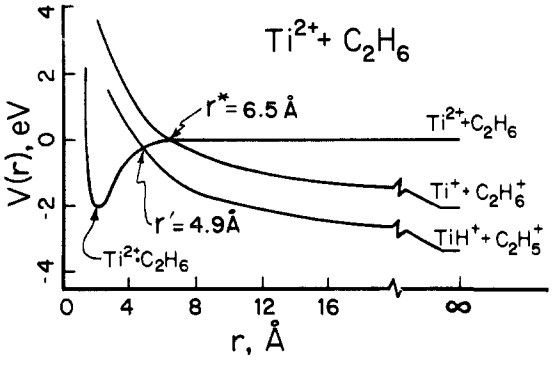

Figure 2. Long-range one-dimensional potentials calculated for the Ti^{2+} + C_2H_6 reaction, showing crossing points for electron transfer (r^*) and hydride transfer (r'). The cluster ion well depth is not known quantitatively.

transfer products TiH^+ + $C_2H_5^+$ almost exclusively (≥90%). No dipositive adduct ion products are observed, but there is some evidence of a small (≤10%) Ti^+ signal. An interesting and rapid secondary reaction is TiH^+ + C_2H_6 → $TiC_2H_5^+$ + H_2, as previously observed by Carlin et al.[10] The Ti^{2+} + C_3H_8 reaction yields ≥70% electron transfer products Ti^+ + $C_3H_8^+$ and ≤30% H^- transfer products TiH^+ + $C_3H_7^+$. All three reactions are fast (Table I).

The one-dimensional potential energy curves of Figure 2, constructed for the C_2H_6 reaction, provide a *qualitative* explanation of the observed reactivity pattern. At long range, reactants Ti^{2+} + RH follow the attractive ion-induced dipole potentil $V_1(r) = -\alpha q^2/r^4$, where α is the RH polarizability and q = +2 is the ion charge.[11] The bimolecular ion pair products from electron transfer or hydride transfer follow the repulsive Coulomb potential $V_2(r) = +q^2/r$ at long range. The product exothermicities, which vary with alkane, control the curve crossing points r^* for electron transfer and r' for hydride transfer. The depth of the Ti^{2+}·RH cluster ion well at short range is unknown.[12]

As Ti^{2+} and RH approach, they first encounter the electron-transfer curve crossing at r^*. The data suggest that for C_2H_6 (r^* = 7.0 Å), the probability of the "electron jump" is <0.1, while for C_3H_8 (r^* = 6.1 Å) it is ≥0.7. If electron transfer does not occur, reactants reach the H^- transfer crossing at r'. Essentially all of the C_2H_6 collisions (r' = 4.6 Å) and the remaining ≤30% of the C_3H_8 collisions (r' = 4.5 Å) hop to the TiH^+ + RH^+ curve and recede to H^- transfer products. The C_2H_6 and C_3H_8 collisions may never sample the short-range cluster ion well. In contrast, the CH_4 collisions avoid both electron transfer (r^* = 14 Å) and H^- transfer (r' = 9.1 Å). The default process is formation of a hot adduct ion that is sufficiently long lived to be stabilized about 15% of the time (the ratio of the effective bimolecular rate constant k, Table I, to the Langevin rate constant k_L) by adduct–He collisions, which occur every 150 ns at 0.38 torr. This Ti^{2+} termolecular reaction is about 70 times more efficient than the Ti^+ + CH_4 association at 0.75 torr.[7] While the adduct ion structures are unknown, $V_1(r)$ is 4 times more attractive for Ti^{2+} than for Ti^+. A more strongly bound Ti^{2+}·CH_4 cluster ion will have a longer lifetime relative to redissociation to reactants.[13] The long-term stability of cold Ti^{2+}·CH_4 relative to electron transfer requires a cluster bond energy >1 eV (Table I).

Earlier studies[14–16] of electron transfer from small neutrals to the closed-shell dipositive ions Mg^{2+}, Ca^{2+}, and Ba^{2+} also show

(10) Carlin, T. J.; Sallans, L.; Cassady, C. J.; Jacobson, D. B.; Freiser, B. S. *J. Am. Chem. Soc.* **1983**, *105*, 6320.
(11) Su, T.; Bowers, M. T. *Int. J. Mass Spectrom. Ion Phys.* **1973**, *12*, 347.
(12) Spears, K. G. *J. Chem. Phys.* **1972**, *57*, 1850.
(13) Meot-ner, M. In *Gas Phase Ion Chemistry*; Bowers, M. T., Ed.; Academic: New York, 1979; Vol. 1. Robinson, P. J.; Holbrook, K. A. *Unimolecular* Reactions; Wiley-Interscience: London, 1972.
(14) Spears, K. G.; Fehsenfeld, F. C. *J. Chem. Phys.* **1972**, *56*, 5698. Spears, K. G.; Fehsenfeld, F. C.; McFarland, M.; Ferguson, E. E. *J. Phys. Chem.* **1972**, *56*, 2562.
(15) Viggiano, A. A.; Howorka, F.; Futrell, J. H.; Davidson, J. A.; Dotan, I.; Albritton, D. L.; Fehsenfeld, F. C. *J. Chem. Phys.* **1979**, *71*, 2734.
(16) Viggiano, A. A.; Fehsenfeld, F. C.; Villinger, H.; Alge, E.; Lindinger, W. *Int. J. Mass Spectrom. Ion Phys.* **1981**, *39*, 1.
(17) Rosenstock, H. M.; Draxl, K.; Steiner, B. W.; Herron, J. T. *J. Pys. Chem. Ref. Data* **1977**, *6*, Suppl. No. 1.
(18) Elkind, J. L.; Ervin, K. M.; Aristov, N.; Armentrout, P. B., unpublished results.
(19) Aue, D. H.; Bowers, M. T. In *Gas Phase Ion Chemistry*; Bowers, M. T., Ed.; Academic: New York, 1979; Vol. 2.

efficient transfer for $r^* < 6$ Å and adduct ion formation whenever electron transfer is slow. The abrupt change from C_3H_8 to C_2H_6 in our work is somewhat surprising, but no account has been taken of possible neutral → ion geometry changes or of chemical forces at short range. The newly observed H^- transfer reaction is inefficient for $r' = 9.1$ Å and highly efficient for $r' = 4.6$ Å, which seems a sensible range dependence for transfer of a heavy particle.

Different pairs of transition-metal ions M^{2+} and organic neutrals can be chosen to systematically vary the exothermicities of certain products and thus the crucial locations of corresponding curve crossings. This will permit considerable control of the product branching. Although M^{2+} species are highly energetic, our initial results indicate that their chemistry will be surprisingly rich and selective.

Acknowledgment is made to the donors of the Petroleum Research Fund, administered by the American Chemical Society, for support of this research and to the National Science Foundation for support under Grant CHE-8302856.

Identification of the Alkaline-Labile Product Accompanying Cytosine Release during Bleomycin-Mediated Degradation of d(CGCGCG)

L. Rabow and J. Stubbe*

Department of Biochemistry, College of Agricultural and Life Sciences, University of Wisconsin-Madison Madison, Wisconsin 53706

J. W. Kozarich and J. A. Gerlt

Department of Chemistry and Biochemistry University of Maryland, College Park, Maryland 20742

Received June 18, 1986

Recent results from our laboratory[1] on the mechanism of DNA degradation by bleomycin (BLM)[2] have allowed us to propose a mechanism for free nucleic acid base release (Figure 1a). This hypothesis is supported by the mechanistic studies from a number of laboratories,[1,3] which indicate that Fe(II) and O_2 or Fe(III) and H_2O_2 can combine with BLM to form "activated BLM", which upon interaction with DNA produces two types of monomeric products, base propenal and free base. While base propenal production[3e] requires activated BLM and additional O_2 and occurs with concomitant DNA strand scission,[3d] the production of base has no additional O_2 requirement and yields strand scission only after treatment with alkali.[3c,i] Our hypothesis predicts that **1** (Figure 1a) is the precursor to this alkali-mediated DNA strand scission. We wish to report that, using the self-complementary hexamer d(CGCGCG) and either Fe(III)·H_2O_2·BLM (anaerobic) or Fe(II)·O_2·BLM, we have identified and quantitated, for the first time, the carbohydrate moiety remaining subsequent to free-base release.[4]

The strategy used to isolate **1** is outlined in Figure 1b. Sodium borohydride trapping of **1** subsequent to isolation by HPLC is an essential feature of the scheme, due to the chemical instability of **1**. A typical reaction mixture containing 0.21 mM Fe(III)·BLM, 0.6 mM H_2O_2, and 0.07 mM double stranded d(CGCGCG) in 10 mM HEPES (pH 7.5) was incubated 1.25 h at room temperature under anaerobic conditions. Analysis of the product distribution by reverse-phase HPLC is shown in Figure 2a. The number of moles of **1** isolated varied between $^1/_3$ to $^1/_2$ the number of moles of cytosine released (Figure 2a, peak A). The material with a retention time of 14 min (**1**) was typically isolated in 35–50% yield and immediately reduced with $NaBH_4$ (NaB^3H_4) at pH 7.6. The reduced reaction product was then chromatographed on both reverse-phase HPLC to give an 88% recovery of **2** (Figure 2b) and anion-exchange Mono Q FPLC to give a 72% yield of a single symmetrical peak.

The material in peak **2** was then subjected to enzymatic digestion with P_1 nuclease and alkaline phosphatase and the resulting products were analyzed by reverse-phase HPLC (Figure 2c). In addition to deoxyguanosine (peak D) (25.5 min) and deoxycytidine (peak C) (17.5 min), an unknown peak with a retention time of 20 min was observed, which contained 1 mol of phosphate per mol of deoxyguanosine and coeluted with the radioactivity. On

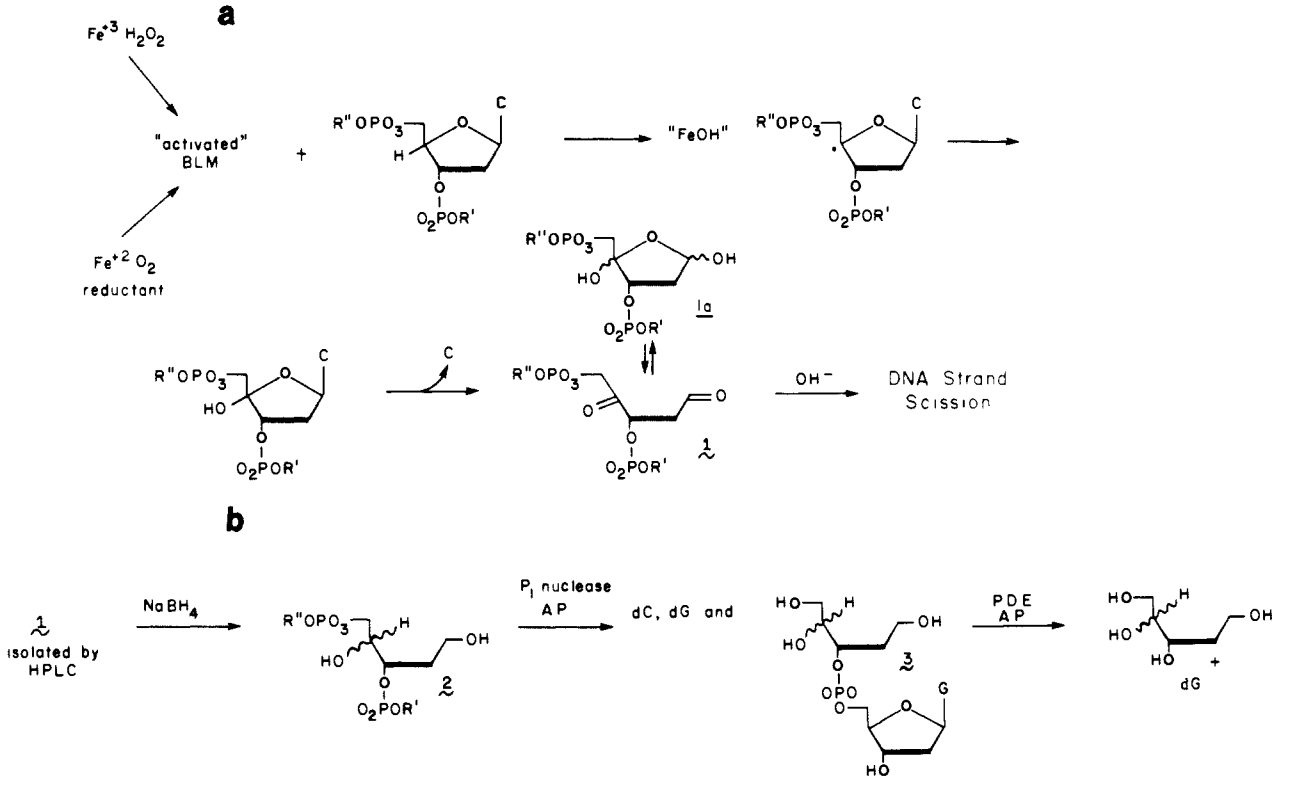

Figure 1. (a) Proposed mechanism for production of alkaline-labile strand scissions mediated by BLM. "FeOH" is a hypothetical hydroxylating species. Compound **1** could be in equilibrium with the ring closed hydrate **1a**.[3g] (b) Protocol for isolation of the carbohydrate moiety produced concomitant with cytosine release. AP, alkaline phosphatase; PDE, phosphodiesterase.

0002-7863/86/1508-7130$01.50/0